

Quantized Distillation: Optimizing Driver Activity Recognition Models for Resource-Constrained Environments

Calvin Tanama[†]Kunyu Peng[†]Zdravko Marinov[†]Rainer Stiefelhagen[†]Alina Roitberg[‡][†]Institute for Anthropomatics and Robotics, Karlsruhe Institute of Technology[‡]Institute for Artificial Intelligence, University of Stuttgart

Abstract—Deep learning-based models are at the top of most driver observation benchmarks due to their remarkable accuracies but come with a high computational cost, while the resources are often limited in real-world driving scenarios.

This paper presents a lightweight framework for resource-efficient driver activity recognition. We enhance 3D MobileNet, a speed-optimized neural architecture for video classification, with two paradigms for improving the trade-off between model accuracy and computational efficiency: knowledge distillation and model quantization. Knowledge distillation prevents large drops in accuracy when reducing the model size by harvesting knowledge from a large teacher model (I3D) via soft labels instead of using the original ground truth. Quantization further drastically reduces the memory and computation requirements by representing the model weights and activations using lower precision integers. Extensive experiments on a public dataset for in-vehicle monitoring during autonomous driving show that our proposed framework leads to an 3-fold reduction in model size and 1.4-fold improvement in inference time compared to an already speed-optimized architecture. Our code is available at <https://github.com/calvintanama/qd-driver-activity-reco>.

I. INTRODUCTION

Efficient models for understanding the situation inside the vehicle cabin have major practical value for both manual and automated driving. During manual driving (SAE¹ levels 1-3), such models can enhance safety through identified distraction or even allow the ADAS system to foresee a dangerous maneuver by analyzing human intent, allowing the system to intervene and prevent accidents [1]. With enhanced automation (SAE levels 4 and 5), they enable a personalized driving experience in the case of autonomous driving, such as situation-aware adjustment of movement dynamics depending on intuitive communication via gestures.

Deep learning approaches deliver excellent results for driver activity recognition [2], [3], [4], [5], [6], [7], but the high computational cost of oftentimes millions of matrix multiplications required for each forward pass is their fundamental weakness and a significant bottleneck for applications within intelligent vehicles, where all sub-systems have to

Emails of the authors: calvin.tanama@student.kit.edu, kunyu.peng@kit.edu, zdravko.marinov@kit.edu, rainer.stiefelhagen@kit.edu, alina.roitberg@f05.uni-stuttgart.de

¹Society of Automotive Engineers, Taxonomy and Definitions for Terms Related to Driving Automation Systems for On-Road Motor Vehicles: https://www.sae.org/standards/content/j3016_202104/

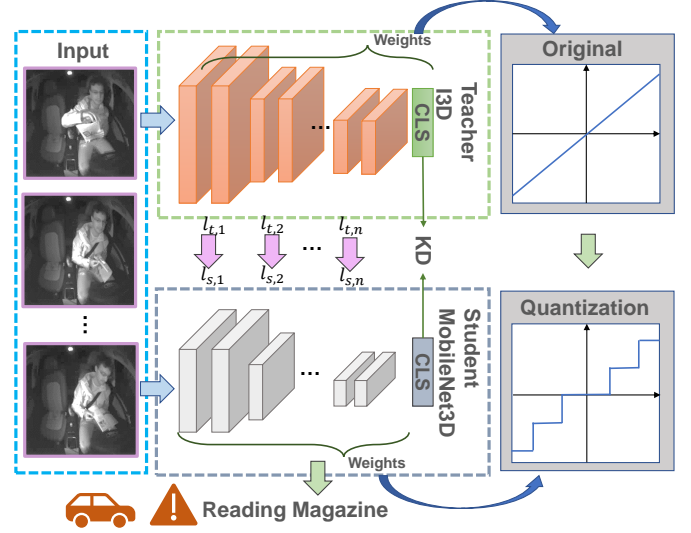


Fig. 1. An overview of our proposed Quantization Distillation (QD) framework for fast driver activity recognition. QD distills the knowledge from the logits of the teacher model (I3D) to the logits of the students model (3D MobileNet), while at the same the weights of the student network are quantized, making the architecture smaller and the inference faster.

share very limited computational and power resources. One way to approach this issue is to utilize architectures based on efficient convolution variants, such as the depthwise separable convolutions within the MobileNet architecture. However, using such lightweight architectures comes with a considerable drop in accuracy compared to a conventional model (I3D), while the CPU inference time (2273.312 ms according to our experiments) might still not be efficient enough for very low-resource environments.

In this paper, we propose a framework for resource-efficient driver activity recognition that addresses the trade-off between accuracy and computational efficiency. We enhance a 3D MobileNet architecture, which is a speed-optimized neural network for video classification, with two paradigms: knowledge distillation and model quantization (overview in Figure 1). The former helps to prevent a large drop in accuracy when reducing the model size by transferring knowledge from a larger teacher model (I3D) via soft labels, while the latter represents the model weights and activations using lower precision integers to reduce memory

and computation requirements. Our extensive experiments on a public dataset for in-vehicle monitoring during autonomous driving show that our proposed framework leads to a significant reduction in model size and inference time compared to an already speed-optimized architecture with only a slight loss in accuracy, making it suitable for deployment in resource-constrained environments.

Overall, our work can be summarized as the following:

- We introduce a framework for resource-efficient driver activity recognition by enhancing the speed-optimized 3D MobileNet architecture with 1) teacher-student knowledge distillation and 2) model quantization. Knowledge distillation transfers knowledge from a larger teacher model (I3D) to a smaller student model (3D MobileNet), while model quantization reduces model size and inference speed by representing model parameters with lower precision integers.
- We conduct extensive experiments on the public Drive&Act dataset for in-vehicle monitoring during autonomous driving using mean per-class accuracy, model size, and inference speed as our metrics. We also examine different properties of the individual building blocks of our models, such as the width multiplier of MobileNet and knowledge distillation hyperparameters.
- We yield a consistent reduction in model size (3-fold) and inference time (1.4-fold) compared to an already speed-optimized 3D MobileNet approach used as our backbone and comparable prediction accuracy obtained through the student-teacher training.

We hope that our work will provide guidance for the architecture design of driver observation models under limited resources and we will make our code publicly available.

II. RELATED WORK

Resource-Efficient Deep Learning. Approaches for making deep learning models more efficient can be broadly divided into three categories: arithmetic, implementation, and model-level techniques [8]. Arithmetic-level approaches aim to reduce the memory footprint and improve data transfer efficiency by utilizing lower precision arithmetic [9], [10]. Implementation-level resource efficiency can be achieved through circuit optimization [11] and spatial architectures [12]. From a model perspective, quantization-based model compression [13], [14], [15], [16], [17], [18], [19], [20], [21], [22] is a well-established technique for reducing the number of bits required by the model. Wu *et al.* [23] and Gong *et al.* [24] leverage k-means scalar quantization to achieve resource reduction from the model parameters. Binary model weights are used for training in BinaryNet [25], BinaryConnect [26], and XNOR networks [27]. Wang *et al.* [28] proposed a learnable lookup table approach for network quantization. Guo *et al.* [29] exploit an adaptive numerical data type for low-bit neural network quantization. A different perspective has been proposed through the advent of differentiable logic gate networks [30]. This approach does not integrate low precision weight quantization. Instead, the structure of these architectures is exclusively built on

logic operations. Model-level resource efficiency can also be achieved through network pruning and sharing [31], [32], [33], [34], [35], [36], [37] and input pruning [38]. Li *et al.* [37] proposed random channel pruning, while Liu *et al.* [39] proposed SOKS, an automatic kernel searching-based approach for strip-wise network pruning. He *et al.* [40] introduced a sparse double dense method while considering model overfitting. In addition to the above-mentioned techniques, knowledge distillation (KD) is a useful training strategy that can produce an efficient model by distilling knowledge from a large-scale model [41], [42], [43], [44], [45], [46]. Our work is inspired by the two aforementioned strategies which we leverage to build a lightweight yet accurate driver activity recognition framework. We enhance a 3D MobileNet architecture often used for driver activity recognition [2], [47], [48] with knowledge distillation and model quantization, which leads to a far better accuracy-efficiency trade-off.

Driver Activity Recognition. Driver activity models can be divided into approaches based on manually designed feature descriptors and end-to-end deep learning approaches which operate directly on video and learn intermediate representations jointly with the classifier. Manual feature-based methods [49], [50], [51], [52], [49], [52] employ classical machine learning techniques, such as Support Vector Machines and Random Forest, with features harvested from driver's hands, body- and head pose, and gaze direction. With the advancement of deep learning techniques, end-to-end deep learning-based models have emerged as a popular approach for driver activity recognition. Convolutional neural networks (CNNs) [2], [3], [4], [5], [6], [7], [53], [54] and transformer-based models [55] are often used as backbones. Despite being an active research area, very few works consider inference time and model size. The common strategy of these approaches is to leverage the speed-optimized architectures, such as MobileNet [56] as their backbones [2], [47], [48]. The work most similar to ours is presumably the recently introduced approach of Li *et al.* [47], where student-teacher distillation is leveraged to improve the lightweight MobileNet model for distracted driver posture identification. In contrast to [47], who propose an image-based approach, we leverage model quantization while our framework operates on video with a spatio-temporal CNN (3D MobileNet) as our backbone. A key ingredient of our approach is the quantization of model weights when training the student-teacher network to speed up the computation, which, to the best of our knowledge, has not been considered yet in the field of driver observation.

III. QUANTIZED DISTILLATION

Our goal is to develop resource-efficient approaches for driver activity recognition. That is, given a video snippet x , our goal is to correctly assign the potentially distractive driver behaviour, while keeping resource demands to a minimum. We begin by employing an already speed-optimized 3D MobileNet architecture as our classification backbone. However, our first experiments reveal two drawbacks of using

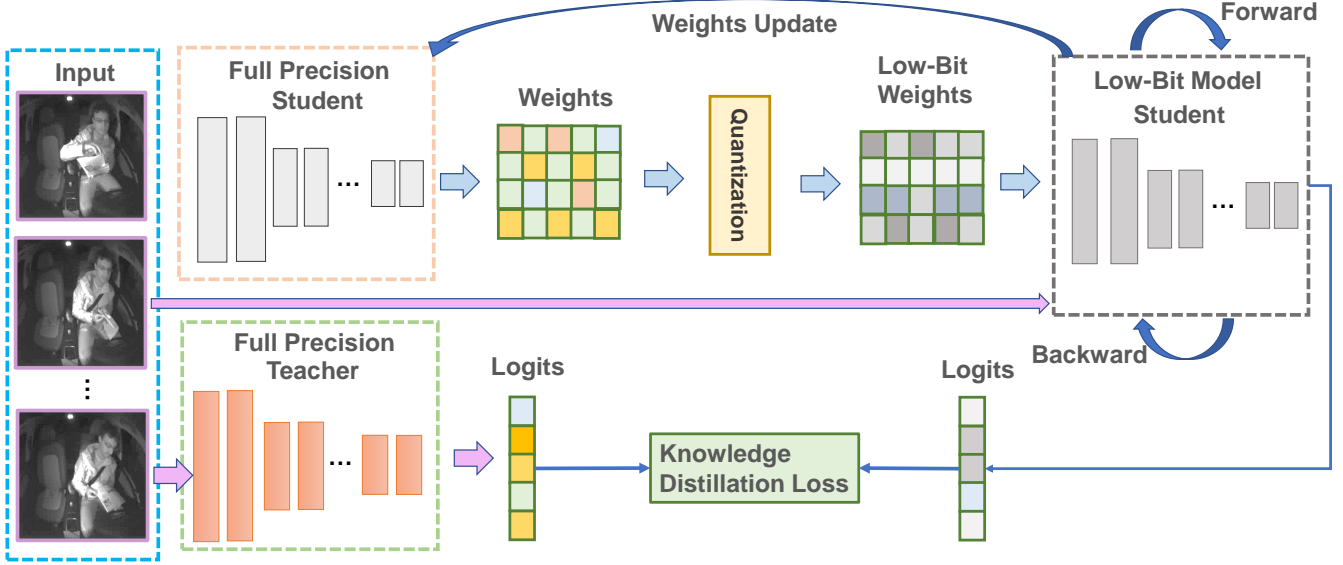


Fig. 2. An overview of the Quantized Distillation training procedure with quantization-aware training. Logit vectors of the accuracy-focused teacher model (I3D) are used for loss computation and training of the lightweight student model (3D MobileNet), yielding higher accuracy than standard training with ground-truth annotations. Note, that quantization of the student weights is carried out post-training, but is also simulated during training.

this model as-is. First, the accuracy of 3D MobileNet is $\sim 20\%$ below the recognition rate of an accuracy-optimized I3D architecture often used in driver observation. Second, despite being much more compact than I3D, even the size of 3 MB might be too large if multiple recognition networks need to share very limited hardware resources. To meet these challenges, we propose a framework based on two paradigms: knowledge distillation and model quantization with quantization-aware training. Knowledge distillation mitigates a decrease in accuracy when optimizing for speed. This is achieved by transferring the knowledge from a larger teacher model (I3D) to a smaller student model (3D MobileNet backbone) through the use of soft labels. We further map the model weights typically represented using 32-bit floating-point numbers to lower precision integers and use quantization-aware training to reduce the amount of memory required for storage and computation.

Next, we will describe the fundamentals of the knowledge distillation mechanism (Section III-A), model quantization and quantization-aware training (Section III-B) used in our framework and introduce the complete Quantized Distillation approach in Section III-C. Finally, in Section III-D, we shed light on the implementation details and the used backbones.

A. Knowledge Distillation

Knowledge distillation (KD) is a technique for training a smaller and simpler model (the student) using a larger and more complex model (the teacher) as a guide [41]. In our case, the teacher model is the I3D network [57], which imparts its knowledge to the smaller MobileNet3D model [58]. The teacher model is trained on the labeled training data $X = \{(x_1, y_1), \dots, (x_N, y_N)\}$ in a supervised manner, and its logits (pre-softmax outputs) for each example x_i are used

as "soft" labels for the student model. The student model f_S is then trained to minimize a KD loss that balances a cross-entropy loss between the student's predictions and the ground truth labels with a knowledge distillation loss that encourages the student to match the teacher's "soft" labels:

$$L_{KD}(f_T, f_S, x_i) = \alpha L_{CE}(y_i, f_S(x_i)) + \beta T^2 L_{CE}(f_T(x_i), f_S(x_i)) \quad (1)$$

Here, α and β are hyperparameters that control the relative weighting of the loss terms, T is a temperature scaling factor that controls the degree of smoothing applied to the predicted probabilities, and L_{CE} is the cross-entropy loss. The soft labels for both teacher and student models are defined as:

$$f_S(x_i)_j = \frac{e^{\frac{z_S(x_i)_j}{T}}}{\sum_n e^{\frac{z_S(x_i)_n}{T}}}, \quad \text{and} \quad f_T(x_i)_j = \frac{e^{\frac{z_T(x_i)_j}{T}}}{\sum_n e^{\frac{z_T(x_i)_n}{T}}} \quad (2)$$

where $z_S(x_i)_j$ and $z_T(x_i)_j$ denote the j -th element of the logits vector for x_i computed by the student and teacher models, respectively. By minimizing the KD loss L_{KD} , the student model learns to produce predictions that are consistent with the teacher's predictions, while still maintaining high accuracy on the ground truth labels.

B. Model Quantization

Model quantization is an effective technique for reducing the memory and computational requirements of deep neural networks. It involves converting continuous values $r \in \mathbb{R}$ to a set of discrete values $q \in \mathbb{Z}$, typically by mapping floating-point numbers to integers. In practice, quantization is achieved through a **quantization scheme** (S, Z) that maps integers q to real numbers r and vice-versa:

$$r = S(q - Z), \text{ and } q = \text{round}\left(\frac{r}{S} - Z\right) \quad (3)$$

where $S \in \mathbb{R}_+$ and $Z \in \mathbb{Z}$ are constant quantization parameters. The zero-point Z corresponds to the quantized value of the real zero, i.e., $r = 0$.

By translating real-number computation into quantized-value computation using the quantization scheme (S, Z) , inference can be performed using only integer arithmetic. We adopt the quantization scheme proposed in [13], which uses the same pair of quantization parameters (S_L, Z_L) for all activation and weight values within each layer L , but different parameters for different layers. For example, a floating-point matrix multiplication $r_3 = r_2 r_1$ used during a forward pass can be quantized using the corresponding parameters $S_\alpha, Z_\alpha, \alpha \in \{1, 2, 3\}$ as (detailed derivation in [13]):

$$q_3^{(i,k)} = Z_3 + 2^{-n} M_0 \sum_{j=1}^N (q_1^{(i,j)} - Z_1)(q_2^{(j,k)} - Z_2) \quad (4)$$

Here, $q_\alpha^{(i,k)}$ is the quantized entry of r_α on the i^{th} row and k^{th} column, $M_0 \in [0.5, 1)$ is a normalized multiplier, and $n \in \mathbb{Z}_+$ is an integer. The multiplication with M_0 is a fixed-point multiplication, while multiplication with 2^{-n} is an efficient bit shift. Overall, model quantization allows us to reduce the memory footprint of deep neural networks and accelerate their inference speed, making them more suitable for deployment on resource-constrained devices.

Quantization Aware Training (QAT). During training, we leverage the QAT technique, which *simulates* 8-bit quantization within the layers [13]. It uses an *observer* to collect statistics of input and output tensors for each layer L to determine its quantization parameters (S_L, Z_L) . *Fake quantization* layers utilize (S_L, Z_L) during forward passes in training to round model parameters in each layer but keep parameters in full precision during backpropagation. QAT optimizes the model's accuracy during inference where **real** quantization is used with fewer parameter bits and integer operations. To avoid zero gradients at quantized values following a "staircase" function, a straight-through estimator (STE) [59] approximates the gradient of the **round**(\cdot) function with the identity function **id**(\cdot), which makes it possible to train directly with quantized weights. *Fused layers* [60] combine bias-addition, activation function evaluation, and quantized matrix multiplication into a single operation. The granularity of fused operators in inference code matches *fake quantization* operators in the training.

Algorithm 1 shows the practical implementation of QAT. It involves loading a model, fusing layers to reduce rounding errors, adding observers and fake quantization, training with STE [59] for gradient computation, and 8-bit quantization of weights, batch normalization, and activations. The model can be calibrated by calculating input/output statistics in the observers. Finally, the model is converted to a quantized model for the desired back-end system.

Algorithm 1 Practical Implementation of QAT

- 1: Load pre-trained/new model
 - 2: Fuse layers
 - 3: Add OBSERVERS and FAKE QUANTIZATION layers
 - 4: Train with STE or calibrate model with OBSERVERS
 - 5: Quantize the model for inference
-

C. Quantized Knowledge Distillation

We propose to combine model quantization with knowledge distillation to produce an efficient 8-bit quantized model, which preserves the knowledge of a larger full-precision teacher model. To achieve this, we interleave the KD-Loss L_{KD} with the QAT from Algorithm 1. This combination can be seen in Algorithm 2

Algorithm 2 Quantized Knowledge Distillation

- 1: Let $f_S :=$ student model, $f_T :=$ teacher model, $X = \{(x_1, y_1), \dots, (x_N, y_N)\} :=$ training data
 - 2: $f_S = \text{fuse_layers}(f_S)$
 - 3: $f_S = \text{add_observers_fake_quantization}(f_S)$
 - 4: **for** $(x_i, y_i) \in X$:
 - 5: Teacher forward pass $f_T(x_i)$
 - 6: Student forward pass $f_S(x_i) \setminus \text{Simulate int8 with QAT}$
 - 7: Compute distillation loss $L_{KD}(f_T, f_S, x_i)$
 - 8: Compute STE student gradient $\nabla_{f_S} = \frac{\partial L_{KD}(f_T, f_S, x_i)}{\partial f_S(x_i)}$
 - 9: Update student $f_S \leftarrow f_S - \eta \cdot \nabla_{f_S}$
 - 10: $f_S \leftarrow \text{convert_to_int8}(f_S)$
 - 11: **return** f_S
-

Algorithm 2 trains a student model f_S using a teacher model f_T to achieve similar performance to the teacher while using only 8-bit quantized weights and activations. First, bias-addition, activations, and matrix multiplications are fused into single operations in f_S to simplify the architecture. Then, we add observers and fake quantization to simulate the effect of 8-bit quantization in f_S during forward passes. For each training example (x_i, y_i) , we compute the forward pass of both the teacher and student models. We then calculate the distillation loss L_{KD} , which measures the discrepancy between the teacher's and student's predictions. The student gradient is calculated using the Straight-Through Estimator (STE) [59], and the student is updated using gradient descent. After training is complete, the student model is converted to 8-bit integers and is used for efficient inference.

The proposed algorithm produces a smaller, more efficient model that retains the knowledge of the larger, more accurate teacher model. By incorporating QAT into the knowledge distillation process, we can optimize for both model size, inference time, and accuracy simultaneously.

D. Implementation Details

I3D. Inflated 3D ConvNet (I3D) [57] is a widely used architecture for video analysis tasks such as action recognition. Initially, based on the Inception V2 architecture, it processes video snippets by "inflating" the original 2D architecture with

an additional temporal dimension. I3D has 27 layers and approximately 25 million parameters.

3D MobileNet. The 3D MobileNet [58] architecture is a variant of the MobileNet architecture designed for 3D video analysis tasks such as action recognition. It consists of depthwise separable convolutions that greatly reduce the number of parameters and computations required by the network, making it suitable for real-time inference on mobile devices and other resource-constrained platforms. An important hyperparameter of MobileNet is the *width multiplier* that controls the number of channels in each layer of the network (smaller width multiplier values lead to a smaller network with fewer parameters).

Training. I3D is pre-trained with the Kinetics-400 dataset and trained for 200 epochs using SGD with learning rate 0.05 and momentum 0.9. The learning rate is scheduled using a multi-step scheduler with a multiplier 0.2 in epochs {70, 100, 150}. Dropout is employed with a probability of 0.5. 3D MobileNet is pre-trained with the Kinetics-600 dataset and trained with the same SGD configuration with additional weight decay of 0.0001 and epoch number as the baseline I3D. For Knowledge Distillation, a fully pre-trained I3D on Drive&Act [3] is used as a teacher and MobileNet pre-trained with Kinetics-600 is used as a student. Student weight α is fixed to $1 - \beta$ with β being the teacher weight. Hyperparameters, *e.g.*, temperature, teacher weight, and width multiplier are tuned and presented in section IV-B. For Quantized Distillation, every Conv-BN-ReLU and Conv-BN module combination are fused. Additionally, batch normalization layers and observers are frozen on epoch 150 and FBGEMM backend [61] is used for integer matrix multiplication. The experiments are implemented using PyTorch version 1.10.2.

Dataset and Data Processing. Drive&Act [3] is a public in-vehicle human activity dataset focused on distractive behavior during both, manual and autonomous driving. The data is collected from 15 subjects and is annotated with 34 fine-grained activities at the main evaluation level. We downsample the videos to a 256×256 resolution and use frame snippets with a size of 16 as input to our model, as required by 3D MobileNet. Segments of the individual activities are usually longer than that, in which case we select the frames randomly, as done in [3]. If the current segment covers fewer frames, zero-valued frames are padded in the end. During training, we use random cropping and horizontal flipping as data augmentation and normalize the values to range [0, 1]. An imbalanced data sampler is used during training to account for the uneven distribution of categories.

IV. EXPERIMENTS

A. Metrics & Benchmark Details

Performance. Following the original evaluation protocol [3], model recognition quality is measured by calculating the mean per class accuracy.

Model Size and Inference Time. Model size is measured by taking the size of the saved model in the form of a .pth file. The inference time for one video data with 16

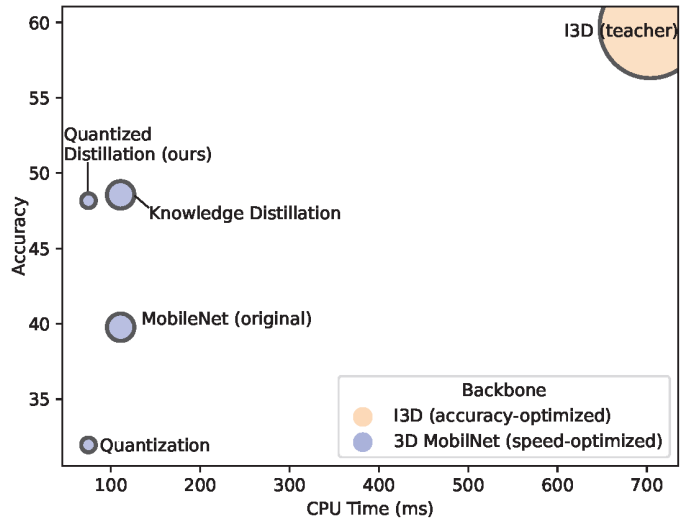


Fig. 3. Comparison of model size, CPU inference time, and accuracy. Model size corresponds to the circle size. The proposed quantized distillation framework yields a good trade-off between accuracy and computational cost.

frames is measured with the PyTorch profiler package by averaging the inference time of 1000 forward pass. The measurement is done on an AMD EPCY 7502P 32-Core CPU. We also mention Floating Point Operations Per Second (FLOPs) for the 3D MobileNet and I3D backbones, but do not use it in the case of the quantized model, where floating point operations are replaced with integer operations, *i.e.*, the total amount of arithmetic operations stays the same, but the integer operations are executed much more efficiently. We, therefore, use the CPU inference time / Frame Per Second (FPS) and the model size as our main metrics.

B. Results

Hyperparameters. We first look at the effect of different hyperparameters on the student-teacher knowledge distillation outcome in Table II: width multiplier of 3D MobileNet and the knowledge distillation hyperparameters temperature T and teacher weight β . All hyperparameter tuning experiments are carried out on the first validation split of Drive&Act. To examine the width multiplier, the temperature, and teacher

TABLE I
EFFECT OF DIFFERENT HYPERPARAMETERS ON THE STUDENT-TEACHER KNOWLEDGE DISTILLATION ACCURACY (FIRST VALIDATION SPLIT).

Width multiplier	T	β	Accuracy (Val 1)
0.5	5	0.7	61.89%
1.0			60.54%
1.5			61.55%
0.5	1	0.7	63.46%
	3		63.49%
	7		60.57%
	9		60.34%
0.5	3	0.5	59.05%
		0.6	61.11%
		0.8	63.93%
		0.9	64.50%
		1.0	62.10%

TABLE II
CLASSIFICATION ACCURACY AND RESOURCE-EFFICIENCY RESULTS

Method	Accuracy [%]						Resource-Efficiency				
	Val 1	Val 2	Val 3	Test 1	Test 2	Test 3	Mean (val)	Mean (test)	Size [MB]	Time [ms]	FPS
Native Architectures & Baselines											
Random chance	2.94	2.94	2.94	2.94	2.94	2.94	2.94	2.94	–	–	–
I3D (accuracy-focused)	67.04	63.7	71.31	60.98	64.93	53.09	67.35	59.67	49.41	703.86	1.42
MobileNet (speed-focused)	49.36	49.09	48.73	36.19	47.02	36.11	49.06	39.77	3.6	107.00	9.34
Optimized Approaches (MobileNet Backbone)											
Knowledge Distillation	64.5	58.73	62.01	49.25	52.11	44.31	61.75	48.56	3.6	107.00	9.34
Quantization	41.48	38.22	40.52	34.2	30.03	31.65	40.07	31.96	1.03	76.79	13.02
Quantized Distillation (ours)	59.78	51.48	61.35	50.11	50.6	43.79	57.54	48.17	1.03	76.79	13.02

TABLE III
CLASSIFICATION ACCURACIES AND DIFFERENCES FOR EACH CLASS

Class	MobileNet [%]	QD (ours) [%]	Δ Acc
closing bottle	37.17	0.0	-37.17
closing door inside	59.89	63.33	+3.44
closing door outside	33.33	88.89	+55.56
closing laptop	9.52	26.19	+16.67
drinking	22.22	23.87	+1.65
eating	21.67	41.48	+19.81
entering car	66.45	77.78	+11.33
exiting car	42.33	71.76	+29.43
fastening seat belt	28.0	78.79	+50.79
fetching an object	21.67	29.72	+8.06
interacting with phone	53.58	40.37	-13.22
looking/moving around	4.76	25.79	+21.03
opening backpack	15.33	2.38	-12.95
opening bottle	12.5	47.44	+34.94
opening door inside	68.33	55.0	-13.33
opening door outside	83.33	93.33	+10.00
opening laptop	39.94	27.55	-12.39
placing an object	0.0	31.87	+31.87
preparing food	0.0	6.67	+6.67
pressing autom. button	93.94	94.18	+0.24
putting laptop in backpack	16.67	0.0	-16.67
putting on jacket	32.29	0.0	-32.29
putting on sunglasses	23.78	38.89	+15.11
reading magazine	43.21	69.82	+26.61
reading newspaper	79.51	80.61	+1.10
sitting still	58.44	81.41	+22.97
taking laptop fr. backpack	50.00	25.00	-25.00
taking off jacket	46.43	70.05	+23.62
taking off sunglasses	4.17	31.21	+27.04
talking on phone	51.96	57.73	+5.77
unfastening seat belt	73.07	64.21	-8.86
using multimedia display	94.1	93.2	-0.90
working on laptop	36.27	67.19	+30.92
writing	24.91	32.01	+7.10

weight are fixed to 5 and 0.7 respectively. The width multiplier 0.5 and 1.5 yield comparable results. Since a lower width multiplier leads to a lower model size, we select 0.5 in the next step. For ablations of the temperature parameter, width multiplier, and teacher weight are fixed to 0.5 and 0.7 respectively and models are trained with varying temperatures of $\{1, 3, 7, 9\}$. With the same evaluation method, temperatures 1 and 3 yield similar results, and the value with the best outcome, *e.g.*, 3 is taken for the next study. For the teacher weight, we consider values of $\{0.5, 0.6, 0.8, 0.9, 1.0\}$, where 0.9 leads to the best outcome (64.5%). It is worth mentioning that for all hyperparameter configurations, student-teacher knowledge distillation training consistently surpasses

the original 3D MobileNet (accuracy of 49.36% on the first validation split, see Table II).

Main Results. Table II summarizes the accuracies and efficiency outcomes of the developed models and baselines for the leading hyperparameter configuration (estimated on the validation set, *i.e.*, width multiplier of 0.5, $T = 3$, $\beta = 0.9$). Looking at the original architectures, the larger I3D model outperforms 3D MobileNet by $\sim 18 - 20\%$ better in terms of test and validation accuracy (averaged over the three splits). This is not surprising due to the much higher capacity of I3D ($13.75\times$ higher model size). The inference time is highly correlated to the number of FLOPs, which is ~ 373.73 MFLOPs and ~ 27832.132 for I3D.

Knowledge distillation with the I3D teacher raises the average accuracy of 3D MobileNet by $\sim 10\%$ on both test and validation sets. As expected, there is still a gap between the average accuracy between I3D and MobileNet with knowledge distillation, as I3D has a far higher number of learnable parameters.

Quantization of 3D MobileNet weights reduces the model size and inference time drastically: the model becomes $\sim 3.5\times$ smaller and $\sim 1.4\times$ faster. This is possible by quantizing all weights and activation values into integers and optimizing integer matrix multiplication used during inference. However, employing quantization without any knowledge distillation reduces the accuracy by $\sim 8\%$ compared to 3D MobileNet. Finally, our complete Quantized Distillation framework raises the recognition quality of quantized 3D MobileNet by $\sim 17\%$ with 57.54% and 48.17% of the validation and test examples classified correctly, surpassing the accuracy of the original MobileNet and nearly reaching the results of the non-quantized MobileNet trained with KD, yet with far better model size and inference time.

Next, we analyze the recognition quality for the individual driver behaviors, comparing our final Quantized Distillation (QD) framework with the original 3D MobileNet (Table III). Despite being much more efficient and smaller in size, QD outperforms the original 3D MobileNet for the vast majority of behavior types. This gain is especially large in categories *closing door outside* and *fastening seat belt* (around 50% increase). However, in 10 (out of 34) total categories, we observed a decline in accuracy, which was considerable for categories *closing bottle* and *putting on jacket* (around 30% loss). Overall, the mean per class accuracy is significantly higher for the proposed KD framework (48.17% vs. 39.77

on the test set, see Table II).

Figure 3 summarizes the trade-off between accuracy and resource efficiency as a scatter graph, with the CPU inference time and accuracy plotted on the X and Y axes respectively, and the model size corresponding to the bubble size. It is worth mentioning, that while the proposed QD framework meets the best accuracy-efficiency trade-off among the lightweight architectures, there is still a 10% gap compared to the large I3D model. While this is expected, as I3D has a large capacity the final model choice should be made depending on the specific requirements of the application.

V. CONCLUSION

In this work, we explored the problem of efficient driver activity recognition aimed at reducing the model size and inference time. To this end, we employed techniques such as quantization and model distillation and studied the effect of different parameters on the recognition performance. We found that these methods can significantly reduce the model size and inference time, while student-teacher knowledge distillation is useful in keeping the loss in accuracy small. In particular, we observed that a combination of quantization and distillation with carefully selected parameters can achieve the best trade-off between accuracy and efficiency. These results suggest that efficient driver activity recognition can be achieved through careful model optimization, and we hope that our study will provide guidance for the development of fast and accurate driver observation models suitable for real-life driving situations.

Acknowledgements. This work was performed on the HoreKa supercomputer funded by the Ministry of Science, Research and the Arts Baden-Württemberg. Kunyu Peng was supported by the SmartAge project sponsored by the Carl Zeiss Stiftung (P2019-01-003; 2021-2026). Alina Roitberg was supported by the Baden-Württemberg Stiftung (Elite Postdoc Program) and Deutsche Forschungsgemeinschaft (DFG) under Germany's Excellence Strategy - EXC 2075.

REFERENCES

- [1] A. Jain, A. Singh, H. S. Koppula, S. Soh, and A. Saxena, "Recurrent neural networks for driver activity anticipation via sensory-fusion architecture," in *ICRA*. IEEE, 2016, pp. 3118–3125.
- [2] D. Tran, H. M. Do, J. Lu, and W. Sheng, "Real-time detection of distracted driving using dual cameras," in *IROS*, 2020.
- [3] M. Martin *et al.*, "Drive&act: A multi-modal dataset for fine-grained driver behavior recognition in autonomous vehicles," in *ICCV*, 2019.
- [4] M. Tan *et al.*, "Bidirectional posture-appearance interaction network for driver behavior recognition," *T-ITS*, 2021.
- [5] A. Roitberg, M. Haurilet, S. Reiß, and R. Stiefelhausen, "CNN-based driver activity understanding: Shedding light on deep spatiotemporal representations," in *ITSC*, 2020.
- [6] A. Roitberg, M. Haurilet, M. Martinez, and R. Stiefelhausen, "Uncertainty-sensitive activity recognition: A reliability benchmark and the CARING models," in *ICPR*, 2021.
- [7] L. Zhao, F. Yang, L. Bu, S. Han, G. Zhang, and Y. Luo, "Driver behavior detection via adaptive spatial attention mechanism," *AEI*, 2021.
- [8] J. Lee, L. Mukhanov, A. S. Molahosseini, U. Minhas, Y. Hua, J. M. del Rincon, K. Dichev, C.-H. Hong, and H. Vandierendonck, "Resource-efficient deep learning: A survey on model-, arithmetic-, and implementation-level techniques," *arXiv preprint arXiv:2112.15131*, 2021.
- [9] D. Xu, M. Xu, Q. Wang, S. Wang, Y. Ma, K. Huang, G. Huang, X. Jin, and X. Liu, "Mandheling: Mixed-precision on-device dnn training with dsp offloading," in *Annual International Conference on Mobile Computing And Networking*, 2022, pp. 214–227.
- [10] Y. Yang, X. Chi, L. Deng, T. Yan, F. Gao, and G. Li, "Towards efficient full 8-bit integer dnn online training on resource-limited devices without batch normalization," *Neurocomputing*, 2022.
- [11] C.-H. Chang, A. S. Molahosseini, A. A. E. Zarandi, and T. F. Tay, "Residue number systems: A new paradigm to datapath optimization for low-power and high-performance digital signal processing applications," *IEEE Circuits and Systems Magazine*, 2015.
- [12] Y.-H. Chen, T. Krishna, J. S. Emer, and V. Sze, "Eyeriss: An energy-efficient reconfigurable accelerator for deep convolutional neural networks," *IEEE Journal of Solid-State Circuits*, vol. 52, no. 1, pp. 127–138, 2017.
- [13] B. Jacob, S. Kligys, B. Chen, M. Zhu, M. Tang, A. Howard, H. Adam, and D. Kalenichenko, "Quantization and training of neural networks for efficient integer-arithmetic-only inference," in *CVPR*, 2018, pp. 2704–2713.
- [14] Y. Cheng, D. Wang, P. Zhou, and T. Zhang, "Model compression and acceleration for deep neural networks: The principles, progress, and challenges," *IEEE Signal Processing Magazine*, vol. 35, no. 1, pp. 126–136, 2018.
- [15] Q. Jin, J. Ren, R. Zhuang, S. Hanumante, Z. Li, Z. Chen, Y. Wang, K. Yang, and S. Tulyakov, "F8net: Fixed-point 8-bit only multiplication for network quantization," *arXiv preprint arXiv:2202.05239*, 2022.
- [16] J. Zhang, Y. Zhou, and R. Saab, "Post-training quantization for neural networks with provable guarantees," *arXiv preprint arXiv:2201.11113*, 2022.
- [17] M. Nagel, M. Fournarakis, Y. Bondarenko, and T. Blankevoort, "Overcoming oscillations in quantization-aware training," in *ICML*. PMLR, 2022, pp. 16 318–16 330.
- [18] Y. Lin, T. Zhang, P. Sun, Z. Li, and S. Zhou, "Fq-vit: Post-training quantization for fully quantized vision transformer," in *IJCAI*, 2022, pp. 1173–1179.
- [19] Z. Yuan, C. Xue, Y. Chen, Q. Wu, and G. Sun, "Ptq4vit: Post-training quantization for vision transformers with twin uniform quantization," in *Computer Vision—ECCV 2022: 17th European Conference, Tel Aviv, Israel, October 23–27, 2022, Proceedings, Part XII*. Springer, 2022, pp. 191–207.
- [20] M. van Baalen, B. Kahne, E. Mahurin, A. Kuzmin, A. Skliar, M. Nagel, and T. Blankevoort, "Simulated quantization, real power savings," in *CVPR*, 2022, pp. 2757–2761.
- [21] Y. Jeon, C. Lee, E. Cho, and Y. Ro, "Mr. biq: Post-training non-uniform quantization based on minimizing the reconstruction error," in *CVPR*, 2022, pp. 12 329–12 338.
- [22] X. Wei, R. Gong, Y. Li, X. Liu, and F. Yu, "Qdrop: randomly dropping quantization for extremely low-bit post-training quantization," *arXiv preprint arXiv:2203.05740*, 2022.
- [23] J. Wu, C. Leng, Y. Wang, Q. Hu, and J. Cheng, "Quantized convolutional neural networks for mobile devices," in *CVPR*, 2016, pp. 4820–4828.
- [24] Y. Gong, L. Liu, M. Yang, and L. Bourdev, "Compressing deep convolutional networks using vector quantization," *arXiv preprint arXiv:1412.6115*, 2014.
- [25] M. Courbariaux and Y. Bengio, "Binarynet: Training deep neural networks with weights and activations constrained to +1 or -1," *CoRR*, vol. abs/1602.02830, 2016. [Online]. Available: <http://arxiv.org/abs/1602.02830>
- [26] M. Courbariaux, Y. Bengio, and J.-P. David, "Binaryconnect: Training deep neural networks with binary weights during propagations," *Advances in neural information processing systems*, vol. 28, 2015.
- [27] M. Rastegari, V. Ordonez, J. Redmon, and A. Farhadi, "Xnor-net: Imagenet classification using binary convolutional neural networks," in *Computer Vision—ECCV 2016: 14th European Conference, Amsterdam, The Netherlands, October 11–14, 2016, Proceedings, Part IV*. Springer, 2016, pp. 525–542.
- [28] L. Wang, X. Dong, Y. Wang, L. Liu, W. An, and Y. Guo, "Learnable lookup table for neural network quantization," in *CVPR*, 2022, pp. 12 423–12 433.
- [29] C. Guo, C. Zhang, J. Leng, Z. Liu, F. Yang, Y. Liu, M. Guo, and Y. Zhu, "Ant: Exploiting adaptive numerical data type for low-bit deep neural network quantization," in *2022 55th IEEE/ACM International Symposium on Microarchitecture (MICRO)*, 2022.

- [30] F. Petersen, C. Borgelt, H. Kuehne, and O. Deussen, "Deep differentiable logic gate networks," *Advances in Neural Information Processing Systems*, vol. 35, pp. 2006–2018, 2022.
- [31] S. Han, H. Mao, and W. J. Dally, "Deep compression: Compressing deep neural networks with pruning, trained quantization and huffman coding," *arXiv preprint arXiv:1510.00149*, 2015.
- [32] S. Hanson and L. Pratt, "Comparing biases for minimal network construction with back-propagation," *Advances in neural information processing systems*, vol. 1, 1988.
- [33] B. Hassibi and D. Stork, "Second order derivatives for network pruning: Optimal brain surgeon," *Advances in neural information processing systems*, vol. 5, 1992.
- [34] D. Blalock, J. J. Gonzalez Ortiz, J. Frankle, and J. Guttat, "What is the state of neural network pruning?" *Proceedings of machine learning and systems*, vol. 2, pp. 129–146, 2020.
- [35] J. Rachwan, D. Zügner, B. Charpentier, S. Geisler, M. Ayle, and S. Günnemann, "Winning the lottery ahead of time: Efficient early network pruning," in *ICML*. PMLR, 2022, pp. 18 293–18 309.
- [36] H. Wang, C. Qin, Y. Bai, Y. Zhang, and Y. Fu, "Recent advances on neural network pruning at initialization," in *IJCAI*, 2022, pp. 23–29.
- [37] Y. Li, K. Adamczewski, W. Li, S. Gu, R. Timofte, and L. Van Gool, "Revisiting random channel pruning for neural network compression," in *CVPR*, 2022, pp. 191–201.
- [38] Z. Marinov, A. Roitberg, D. Schneider, and R. Stiefelhofen, "Mod-select: Automatic modality selection for synthetic-to-real domain generalization," in *Computer Vision–ECCV 2022 Workshops: Tel Aviv, Israel, October 23–27, 2022, Proceedings, Part VIII*. Springer, 2023, pp. 326–346.
- [39] G. Liu, K. Zhang, and M. Lv, "Soks: Automatic searching of the optimal kernel shapes for stripe-wise network pruning," *IEEE Transactions on Neural Networks and Learning Systems*, 2022.
- [40] Z. He, Z. Xie, Q. Zhu, and Z. Qin, "Sparse double descent: Where network pruning aggravates overfitting," in *ICML*. PMLR, 2022, pp. 8635–8659.
- [41] G. Hinton, O. Vinyals, and J. Dean, "Distilling the knowledge in a neural network," *arXiv preprint arXiv:1503.02531*, 2015.
- [42] L. Zhang, X. Chen, X. Tu, P. Wan, N. Xu, and K. Ma, "Wavelet knowledge distillation: Towards efficient image-to-image translation," in *CVPR*, 2022, pp. 12 464–12 474.
- [43] R. He, S. Sun, J. Yang, S. Bai, and X. Qi, "Knowledge distillation as efficient pre-training: Faster convergence, higher data-efficiency, and better transferability," in *Proceedings of the IEEE/CVF Conference on Computer Vision and Pattern Recognition*, 2022, pp. 9161–9171.
- [44] X. Chen, Q. Cao, Y. Zhong, J. Zhang, S. Gao, and D. Tao, "Deardk: data-efficient early knowledge distillation for vision transformers," in *CVPR*, 2022, pp. 12 052–12 062.
- [45] R. Liu, K. Yang, A. Roitberg, J. Zhang, K. Peng, H. Liu, and R. Stiefelhofen, "Transkd: Transformer knowledge distillation for efficient semantic segmentation," *arXiv preprint arXiv:2202.13393*, 2022.
- [46] J. Zhang, C. Chen, J. Dong, R. Jia, and L. Lyu, "Qekd: query-efficient and data-free knowledge distillation from black-box models," *arXiv preprint arXiv:2205.11158*, 2022.
- [47] W. Li, J. Wang, T. Ren, F. Li, J. Zhang, and Z. Wu, "Learning accurate, speedy, lightweight cnns via instance-specific multi-teacher knowledge distillation for distracted driver posture identification," *IEEE Transactions on Intelligent Transportation Systems*, vol. 23, no. 10, pp. 17 922–17 935, 2022.
- [48] J. D. Ortega, N. Kose, P. Cañas, M.-A. Chao, A. Unnervik, M. Nieto, O. Otaegui, and L. Salgado, "Dmd: A large-scale multi-modal driver monitoring dataset for attention and alertness analysis," in *Computer Vision–ECCV 2020 Workshops: Glasgow, UK, August 23–28, 2020, Proceedings, Part IV 16*. Springer, 2020, pp. 387–405.
- [49] E. Ohn-Bar, S. Martin, A. Tawari, and M. M. Trivedi, "Head, eye, and hand patterns for driver activity recognition," in *ICPR*, 2014.
- [50] L. Xu and K. Fujimura, "Real-time driver activity recognition with random forests," in *AutomotiveUI*, 2014.
- [51] R. Zheng, K. Nakano, H. Ishiko, K. Hagita, M. Kihira, and T. Yokozeki, "Eye-gaze tracking analysis of driver behavior while interacting with navigation systems in an urban area," *THMS*, 2016.
- [52] C. Braunagel, E. Kasneci, W. Stolzmann, and W. Rosenstiel, "Driver-activity recognition in the context of conditionally autonomous driving," in *ITSC*, 2015.
- [53] A. Roitberg, K. Peng, Z. Marinov, C. Seibold, D. Schneider, and R. Stiefelhofen, "A comparative analysis of decision-level fusion for multimodal driver behaviour understanding," in *2022 IEEE Intelligent Vehicles Symposium (IV)*. IEEE, 2022, pp. 1438–1444.
- [54] A. Roitberg, K. Peng, D. Schneider, K. Yang, M. Koulakis, M. Martinez, and R. Stiefelhofen, "Is my driver observation model overconfident? input-guided calibration networks for reliable and interpretable confidence estimates," *IEEE Transactions on Intelligent Transportation Systems*, vol. 23, no. 12, pp. 25 271–25 286, 2022.
- [55] K. Peng, A. Roitberg, K. Yang, J. Zhang, and R. Stiefelhofen, "Transdarc: Transformer-based driver activity recognition with latent space feature calibration," in *IROS*. IEEE, 2022, pp. 278–285.
- [56] A. G. Howard, M. Zhu, B. Chen, D. Kalenichenko, W. Wang, T. Weyand, M. Andreetto, and H. Adam, "Mobilenets: Efficient convolutional neural networks for mobile vision applications," *arXiv preprint arXiv:1704.04861*, 2017.
- [57] J. Carreira and A. Zisserman, "Quo vadis, action recognition? A new model and the kinetics dataset," in *CVPR*, 2017.
- [58] O. Kopuklu, N. Kose, A. Gunduz, and G. Rigoll, "Resource efficient 3d convolutional neural networks," in *ICCV Workshops*, 2019.
- [59] S. K. Esser, J. L. McKinstry, D. Bablani, R. Appuswamy, and D. S. Modha, "Learned step size quantization," *arXiv preprint arXiv:1902.08153*, 2019.
- [60] B. Jacob and P. Warden, "gemmlowp: A small self-contained low-precision gemm library," *Retrieved June*, vol. 14, p. 2018, 2017.
- [61] D. Khudia, J. Huang, P. Basu, S. Deng, H. Liu, J. Park, and M. Smelyanskiy, "Fbgemm: Enabling high-performance low-precision deep learning inference," *arXiv preprint arXiv:2101.05615*, 2021.